# THE GROWTH OF SMALL CORROSION FATIGUE CRACKS IN ALLOY 7075

R.S. Piascik*

The corrosion fatigue crack growth characteristics of small (>35µm) surface and corner cracks in aluminum alloy 7075 is established. The early stage of crack growth is studied by performing *in situ* long focal length microscope (500X) crack length measurements in laboratory air and 1% NaCl environments. To quantify the "small crack effect" in the corrosive environment, the corrosion fatigue crack propagation behavior of small cracks is compared to long through-the-thickness cracks grown under identical experimental conditions. In salt water, long crack constant $K_{max}$ growth rates are similar to small crack da/dN.

## INTRODUCTION

The propagation of small fatigue cracks from surface defects (5 µm to 10 µm) constitutes a large percentage (50% to 90%) of the total fatigue life of structural components (Newman et al (1)). Thus, accurate prediction of small crack da/dN is required for damage tolerant based life predictions. A problem arises because small cracks propagate at unpredictable accelerated rates compared to long fatigue cracks (Ritchie and Lankford (2)). The difference in long and small crack growth behavior is due to numerous effects; for example, diminished crack-tip shielding (closure) effects at small crack sizes. Compounding the small crack problem are complex environmental effects. Research on high strength steels in salt water has shown that chemically-short (< 500µm) cracks propagate 1.5 to 500 times faster than long cracks subjected to the same mechanical driving force (Gangloff and Wei (3)). Limited data on 2000 series alloys exposed to deaerated salt water suggest little chemical-crack-length effect (Piascik and Willard (4)). The aim of this work is to study the chemical crack length effect in environmentally sensitive alloy 7075-T6.

* NASA-Langley Research Center, Hampton, Virginia 23681-0001 USA

# EXPERIMENTAL PROCEDUES

Constant amplitude fatigue crack growth experiments were conducted using a pin loaded extended compact tension (ECT) specimen (also known as the eccentrically loaded single edge cracked tension specimen) as shown in Figure 1. The blunt notched alloy 7075-T6 sheet specimens were oriented in the longitudinal – transverse (L-T) direction. The growth of small surface and corner cracks located at the root of the polished (through 0.3 μm diamond paste) blunt notch were monitored *in situ* by using the long focal length (X500 magnification) microscope shown in Figure 2. The surface crack length (a) was measured to an accuracy of approximately 3 μm in air and 5 μm in salt water. The acetate replica method (Swain (5)) was also used to verify microscope based surface dimension of small cracks at the root of the notch. Crack length measurements were conducted while the specimen remained at 70% of maximum load. Small surface and corner crack growth rates and stress intensity factors were calculated assuming uniform semicircular crack geometry and procedures documented elsewhere (Piascik and Willard (4)).

Small crack experiments in laboratory air were conducted at constant $\Delta P$ and stress ratio (R) of 0.05 with a minimum crack length resolution of 35 μm. All corrosion fatigue tests were performed using the similar loading history; crack initiation was performed at constant $\Delta P$ (R = 0.05) and small crack growth testing was conducted at low and high R by varying $P_{min}$ at constant $P_{max}$. Constant $P_{max}$ testing eliminated possible load history effects when varying $\Delta K$. Reduced *in situ* crack length measurement resolution limited the study of corrosion fatigue cracks to a ≥ 100 μm and to high R (0.7≤ a ≤0.8) testing for the investigation of low $\Delta K$ environmental da/dN.

The direct current electrical potential drop method was used to monitor the growth of through-the-thickness cracks. The computer controlled long crack experiments were conducted by continuously adjusting the load to maintain the programmed $\Delta K$ and R. The decreasing $\Delta K$ test was conducted at variable R (0.2 ≤ R ≤0.09) at a constant $K_{max}$ (15 MPa√m).

A 1.5 litre O-ring sealed plastic chamber, shown in Figure 2, was used for salt-water corrosion fatigue experiments. The mid-half of the ECT specimen was continuously immersed in helium deaerated 1% NaCl (pH = 8) solution. All aqueous NaCl experiments were conducted at constant electrode potential using a potentiostat, two fully immersed platinum counter electrodes and a Ag/AgCl reference electrode. All deaerated corrosion fatigue experiments were conducted at a constant electrochemical potential of -830 $mV_{SCE}$ (approximately 100 $mV_{SCE}$ cathodic of the breakaway or pitting

potential). The distilled water/salt solution was continuously circulated through the test chamber at a rate of 30 ml/min. from a reservoir containing 25 l of argon deaerated NaCl solution. A quartz window located on the side of the chamber and adjacent to the notch was used for *in situ* long focal length microscope viewing of the notch root surface fatigue cracks.

## EXPERIMENTAL RESULTS AND DISCUSSION

### Fatigue Crack Growth Rate

Figure 3 shows the crack growth characteristics of small surface and corner cracks in air at R = 0.05. Here, data are shown for a range of crack lengths, 10 $\mu$m $\leq$ a $\leq$ 1000 $\mu$m for replica based measurements and 35 $\mu$m $\leq$ a $\leq$ 1400 $\mu$m for microscope based measurements. Typical of small crack data, the scatter is presumed to be a result of crack-front/microstructure interaction (Ritchie and Lankford (2)). A power law fit of the microscope and replica data (solid and dotted lines, respectively) show that both measurement techniques yield nearly identical small crack da/dN for alloy 7075. Further comparisons with literature small crack data (dashed line power law fit) for similar low R (R=0) show that the ECT results correlate well with replica based data from single edge notch tests (Newman et al (6)). Long crack growth characteristics (R=0) are similar to small crack da/dN for $\Delta$K>3 MPa$\sqrt{m}$, but small cracks exhibit accelerated da/dN in the long crack growth threshold regime.

The results in Figure 4 show that small cracks ranging in size from 100 $\mu$m to 1400 $\mu$m exhibit accelerated fatigue crack growth rates in deaerated 1% NaCl compared to laboratory air at a loading frequency of 5 Hz. A comparison of the salt water and air power law fit (solid and dashed lines, respectively) show that fatigue crack growth rates are accelerated by a factor of three in NaCl. The corrosion fatigue crack propagation behavior of small cracks is also compared to long crack da/dN in Figure 4. Long crack growth rates at a constant $K_{max}$= 15 MPa$\sqrt{m}$ are essentially closure free, accelerated compared to R = 0.1 da/dN, and envelop the majority of small crack data; similar small and long crack behavior in deaerated salt-water suggests no crack length chemical effect. The increase in long crack constant $K_{max}$ and R da/dN for $\Delta$K>7 MPa$\sqrt{m}$ may be a result of stress corrosion cracking effects.

### Small Crack Fractography

Figure 5 shows the region of crack initiation and the typical morphology of a semicircular shaped corrosion fatigue surface crack (a = 355 $\mu$m) that was exposed to deaerated NaCl (-800 mV). The micrographs are oriented normal to the fatigue crack surface and the surface of the blunt notch is located at the

bottom of both micrographs. The fatigue crack initiated at a corrosion pit located at the root of the blunt notch (arrow shown in Figure 5a). Following initiation, the crack propagated along a transgranular semicircular shaped crack path marked by the dashed lines in Figure 5a. The high magnification micrograph in Figure 5b shows that the fatigue crack initiated at a corrosion pit approximately 10 μm in depth. The pit is elongated in shape with microcrack like features emanating from the region of greatest pit depth. Figure 6 shows typical examples pit surface morphology. The micrographs in Figure 6 are oriented normal to the corroded blunt notch surface and in the highly stressed region very near the fatigue crack. Here, both micrographs show that surface pits, 10 μm to 20 μm in size, contain regions of microcracking. The pit shown in Figure 6b exhibits a microcrack-like morphology similar to the subsurface pit morphology observed in Figure 5b.

## CONCLUSIONS

No chemical crack length effect was observed. For deaerated salt-water solution, small surface and corner fatigue cracks exhibited similar crack growth rates as those observed for long though-the-thickness cracks. Small cracks exposed to salt-water exhibit a factor of three increase in da/dN compared to small crack growth rates in air. A similar factor of three increase in long crack da/dN (R=0.1) was observed in NaCl compared to long crack growth rates (R=0.05) in air. Presumably, small crack growth rate data shown herein was truncated near a $\Delta K = 1$ MPa$\sqrt{m}$ due to crack length resolution. It is likely that small cracks grow at accelerated rates for $\Delta K < 1$ MPa$\sqrt{m}$.

## REFERENCES

(1) Newman, J, Jr., Phillips, E., Swain, M., and Everett, R., Jr., ASTM STP 1122, 1992, pp. 5-27.

(2) "Small Fatigue Cracks", Edited by R.O. Ritchie and J. Lankford, TMS-AIME, Warrendale, PA, 1986.

(3) Gangloff, R. and Wei, R., in Ref. 2, pp. 239-264.

(4) Piascik, R. and Willard, S., J. Fat. Fract. Engng. Mater. Struct., Vol. 17, No.11, 1994, pp. 1247-1259.

(5) Swain, M., ASTM STP 1149, 1992, pp. 34-56.

(6) Newman, J., Jr., Wu, X., Venneri, S., and Li, C., "Small Crack Effects in High-Strength Al Alloys", 1994, NASA RP 1309, NASA, Hampton, VA.
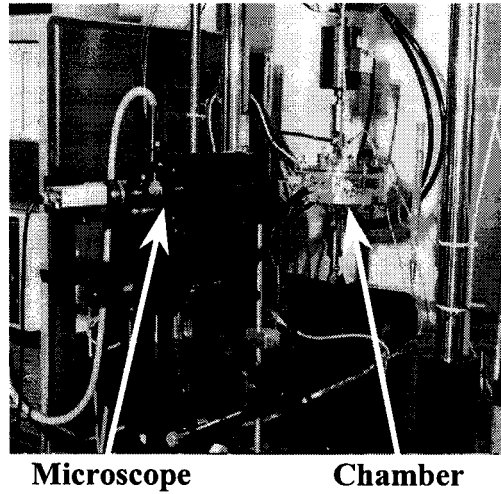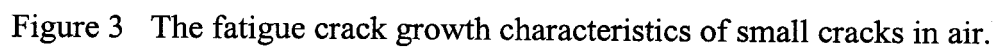
Figure 1  ECT specimen



Microscope          Chamber

Figure 2  Corrosion fatigue setup



Figure 3   The fatigue crack growth characteristics of small cracks in air.
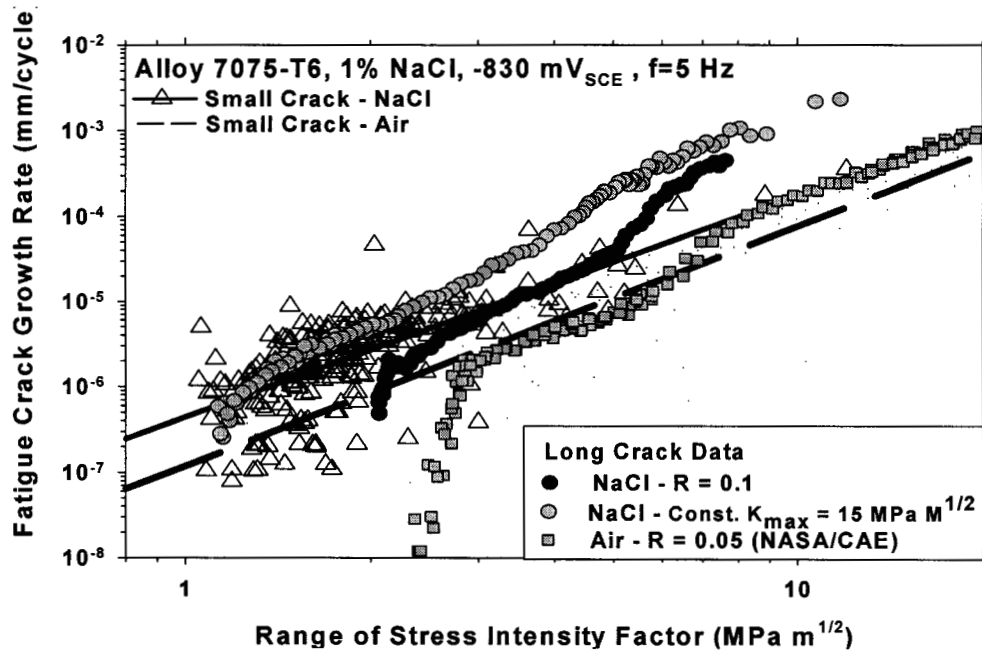
Figure 4   The corrosion fatigue crack growth characteristics of small and long cracks in deaerated salt water.
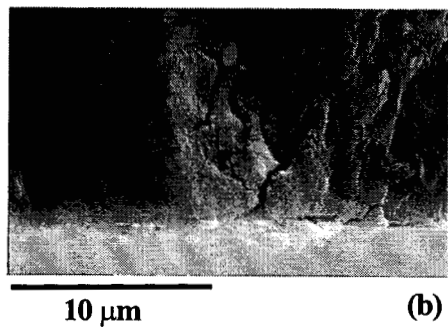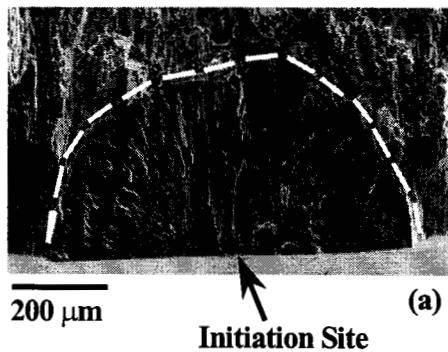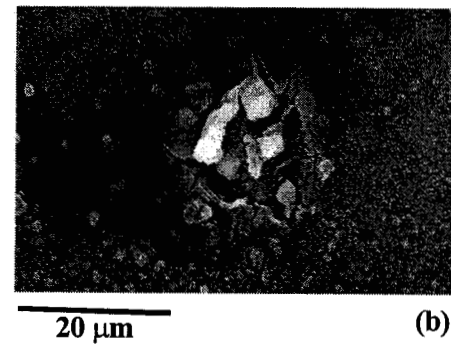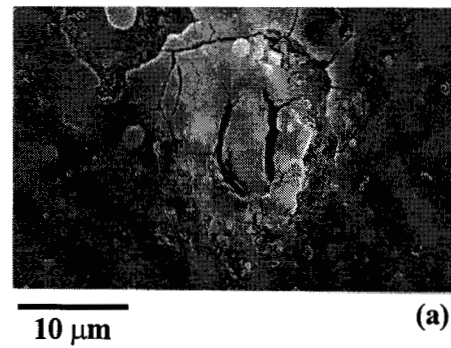


Figure 5  Fatigue crack/initiation



Figure 6  Surface pitting